Environmental Science & Technology

pubs.acs.org/est

Article

Glacier Melt Enhances Suspended Sediment and Mercury Export from the Tibetan Plateau

Mingyue Li, Dongfeng Li,* Xuejun Sun, Jon R. Hawkings, Jeroen E. Sonke, Yanxu Zhang, and Qianggong Zhang

Cite This: Environ. Sci. Technol. 2026, 60, 14150−14160

Read Online

ABSTRACT: Glacier-fed streams (GFSs) export large amounts of suspended sediment (SS) and associated mercury, with important implications for downstream water quality, yet the controls on Hg export remain poorly constrained. This issue is particularly acute on the Tibetan Plateau, where glacier meltwater sustains major Asian rivers. Here, we quantify seasonal and diurnal variability (n = 350) in SS and Hg across six Tibetan Plateau GFSs and synthesize observations from 36 GFSs worldwide. Tibetan Plateau GFSs exhibit total Hg (THg) concentrations and yields comparable to Alaska, but higher than most GFSs with similar glacier coverage. In GFSs without proglacial lakes, THg export scales with SS and increases with glacier coverage and velocity, indicating mobilization of erosion-derived, particle-associated Hg. THg−SS hysteresis differs among glacier thermal regimes in response to particle sorting and subglacial drainage evolution. Our results suggest that intensifying melt and rainfall on the Tibetan Plateau may increase Hg yields and delay the timing of peak Hg export, whereas expanding proglacial lakes may temporarily buffer further downstream Hg export. This study identifies controls on SS and THg export in Tibetan Plateau GFSs and highlights implications for downstream water quality and ecosystem exposure under glacier retreat.

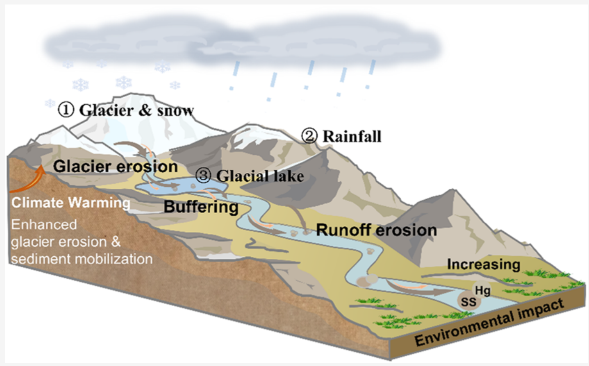

KEYWORDS: *Tibetan Plateau, glacier meltwater, mercury export, climate change*

INTRODUCTION

Mercury is a pervasive global pollutant that, once transformed into the neurotoxic methylmercury (MeHg), poses substantial risks to ecosystems and human health.[1] Anthropogenic activities, primarily coal combustion, gold mining, and industrial manufacturing, have increased Hg loading to aquatic environments,[2,3] and contemporary riverine Hg fluxes are estimated to be two to three times higher than preindustrial levels.[3] Although global anthropogenic Hg emissions have declined in recent decades, substantial legacy Hg persists in the environment.[4,5] Both this legacy and naturally occurring Hg may be remobilized under climate change, especially in warming-sensitive cryospheric environments.[6,7]

Hg from both natural and anthropogenic sources can be transported over long distances and subsequently deposited and stored in glacier ice and snowpacks.[8,9] Glaciers therefore act as important reservoirs and processors of this deposited Hg.[10,11] For example, Arctic glaciers are estimated to store ~2400 Mg of Hg, compared with 1870 Mg in the Arctic Ocean.[12] Glaciers also promote physical and chemical erosion of underlying bedrock, sediment, and paleosols, producing fine particles, known as glacial flour, that can scavenge Hg and facilitate downstream transport during melt.[13,14] As glaciers melt and retreat, both ice-stored Hg and subglacially derived Hg may be exported to glacier-fed streams (GFSs), potentially altering exposure regimes in downstream ecosystems.[15−17] Intensified subglacial erosion, enhanced terrestrial runoff, and more frequent extreme precipitation events may further alter the physical and biogeochemical conditions of downstream freshwater systems,[18,19] promoting Hg mobilization and export. In addition, inputs of terrestrial organic matter (OM) and sulfate (SO_4^{2-}) to proglacial zones may stimulate Hg methylation in surface waters and sediments, amplifying ecological risks.[20,21] Recent studies have linked glacial meltwater-driven erosion and sediment transport to increased Hg export in the pan-arctic Yukon River basin, along the southwestern margin of the Greenland Ice Sheet, and within a fjord of West Antarctica.[9,19,22] However, evidence remains uneven across glacierized regions, with most observations derived from single catchments, sparse sampling, and limited contrasts in glacier thermal and hydrological regimes. As a

Received: January 25, 2026
Revised: April 29, 2026
Accepted: April 29, 2026
Published: May 7, 2026

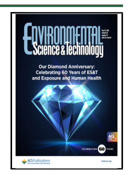

https://doi.org/10.1021/acs.est.6c01369
Environ. Sci. Technol. 2026, 60, 14150−14160

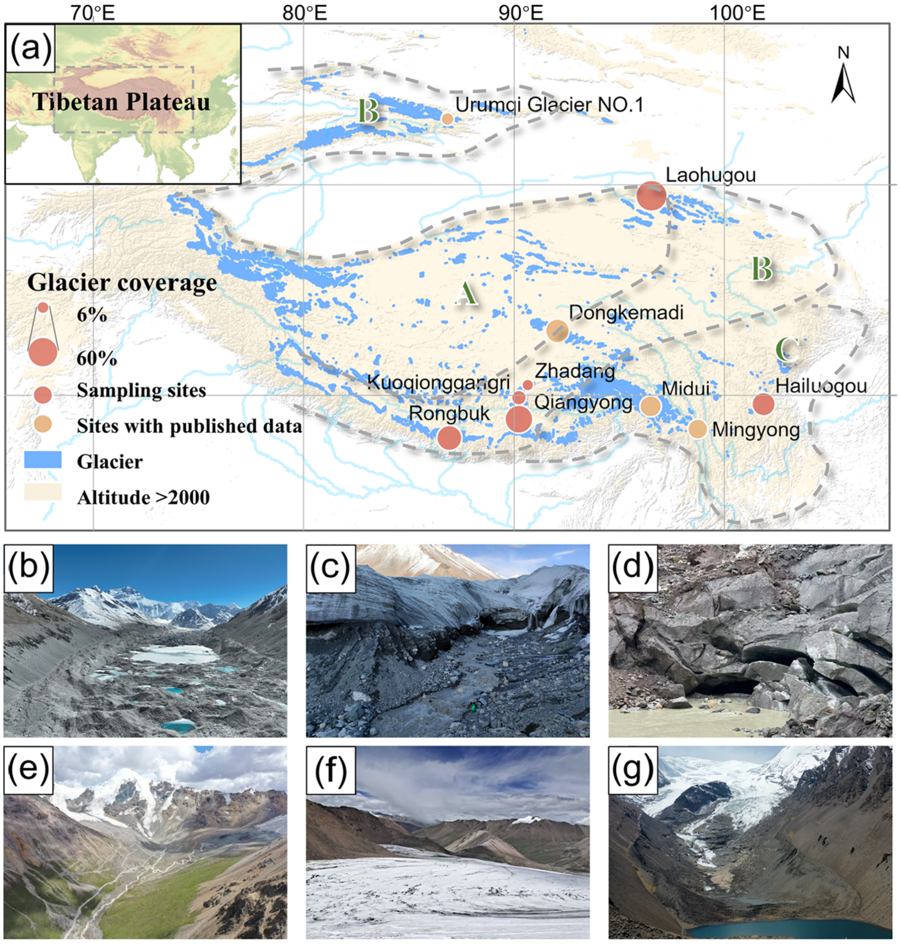

Figure 1. Study area and glacier settings of six glacier-fed streams (GFSs) across the Tibetan Plateau. (a) Locations of sampling sites analyzed in this study (red circles) and published sites used for comparison (orange circles). Symbol size indicates glacier coverage within each catchment. Dashed lines indicate regions with different glacier thermal regimes: extremely continental glaciers (Region A), subcontinental glaciers (Region B), and temperate glaciers (Region C). (b–g) Representative photographs of the studied GFSs: Rongbuk (b), Laohugou (c), Hailuogou (d), Kuoqionggangri (e), Zhadang (f), and Qiangyong (g). Additional site information is provided in Table S1.

result, the controls on Hg export across diverse glacierized catchments remain insufficiently constrained.

The Tibetan Plateau and its surrounding areas, often referred to as the "Third Pole" and the "Asian Water Tower,"[23] host the largest glacierized area outside the Arctic and Antarctic. Accelerated warming has resulted in glacier mass loss of 21.1 ± 5.2 Gt yr^{-1} during 2000–2019.[24] Meltwater from these glaciers sustains the headwaters of 13 major Asian rivers,[23,25] making this fragile region a potentially important yet underexplored hotspot of environmental Hg cycling and exposure.[7] In riverine systems, suspended sediment (SS) is a major vector of Hg transport, with particulate Hg (pTHg) typically dominating the total Hg (THg) load.[26,27] On the Tibetan Plateau, glacier melt exerts primary control on SS export,[18] and SS yields are projected to more than double by 2050 under extreme warming and wetting scenarios.[28] Yet the trajectory of riverine Hg under accelerating glacier retreat remains uncertain,[12] and the mechanisms by which glacial and climatic variability jointly regulate sediment dynamics and Hg mobility in GFSs are poorly understood. The Tibetan Plateau spans diverse glacier types, bedrock lithologies, and strong climatic gradients, providing a unique natural laboratory for addressing these gaps.

Here, we investigate seasonal and diurnal variability of SS and Hg across six GFSs on the Tibetan Plateau (Figure 1) to characterize their spatiotemporal patterns and environmental drivers. We assess the relative roles of glacier melt, precipitation, and ice velocity in regulating SS and Hg export across catchments with contrasting glacier types and geological settings. By integrating hourly and monthly field observations with meteorological and cryospheric data sets, we develop a process-based framework linking SS and THg dynamics in GFSs to evaluate how ongoing glacier retreat may reshape Hg export from high mountain headwaters. Our results provide observational constraints on climate-driven reorganization of Hg transport and highlight the importance of incorporating cryospheric processes into future assessments of riverine Hg exposure.

■ MATERIALS AND METHODS

Study Area

The Tibetan Plateau hosts the largest glacierized area outside the polar regions, with more than 77,000 glaciers covering approximately 83,350 km^2.[23] Under ongoing climate warming, these glaciers have experienced accelerated mass loss.[24] Based on climate setting and thermal regime, glaciers on the Tibetan Plateau are commonly classified as subcontinental, extremely continental, and temperate

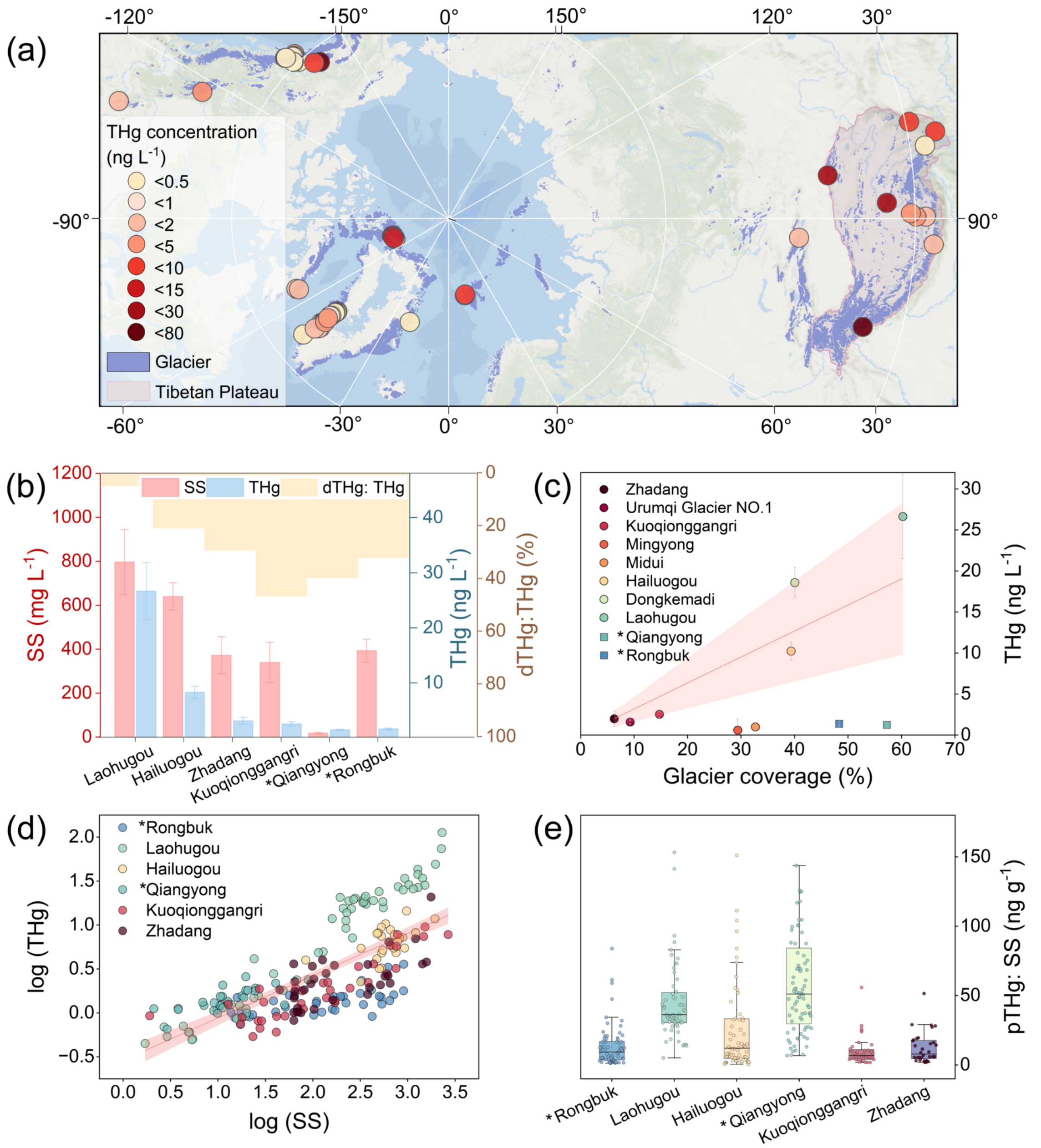

Figure 2. Spatial variability in suspended sediment (SS), total mercury (THg), and glacier influence across GFSs on the Tibetan Plateau. (a) Comparison of THg concentrations in Tibetan Plateau GFSs and other reported GFSs worldwide. All data are provided in Table S2. (b) Monsoon-season mean SS, THg, and dissolved fraction (dTHg: THg) across six Tibetan Plateau catchments. Catchments with upstream proglacial lakes are marked with *. (c) Relationship between THg concentration and glacier coverage. The linear regression was fitted with the intercept fixed at zero ($y = 0.32x$, $R^2 = 0.77$, $p < 0.01$); lake-influenced catchments deviate from this trend. (d) Log−linear relationship between THg and SS concentrations across the six GFSs ($y = 0.48x - 0.54$, $R^2 = 0.54$, $p < 0.01$). (e) Variability in SS-normalized THg (THg: SS) among the six GFSs.

types.[29,30] Continental glaciers generally occur in colder, drier regions where precipitation is below 1000 mm and relatively slow ice flow, whereas temperate glaciers occur under warmer and wetter conditions and tend to exhibit more dynamic flow. Across the Tibetan Plateau, mean annual air temperature ranges from −4.9 to 6.1 °C, and precipitation shows a pronounced southeast-northwest gradient. Approximately 60−90% of annual precipitation falls during the monsoon season from June to September. The southeastern Plateau receives substantially higher annual precipitation, averaging 866 ± 237 mm, whereas the arid northwestern region receives 311 ± 86 mm. We investigated six GFSs distributed across this climatic gradient and spanning elevations from 2920 to 5300 m. Site locations, sampling periods, and catchment lithology are summarized in Table S1.

Mercury and Sediment Data

To characterize seasonal variability in SS and Hg, we collected river water samples 4−5 times per month during 2019−2020 from three representative catchments with contrasting glacier types, including Laohugou, an extremely continental glacier, with 54 samples ($n = 54$); Rongbuk, a subcontinental glacier ($n = 73$); and Hailuogou, a temperate glacier ($n = 72$). These catchments were selected because observation stations near the glacier termini enabled regular sampling and continuous acquisition of long-term meteorological data. All monthly samples were collected at approximately 12:00 local time to minimize the influence of diurnal variability. To characterize short-term variability associated with daily glacier melt cycles, we conducted high-resolution sampling at 2 h intervals for 2−3 days during the peak melt season from June to September in three additional subcon-

https://doi.org/10.1021/acs.est.6c01369
Environ. Sci. Technol. 2026, 60, 14150−14160

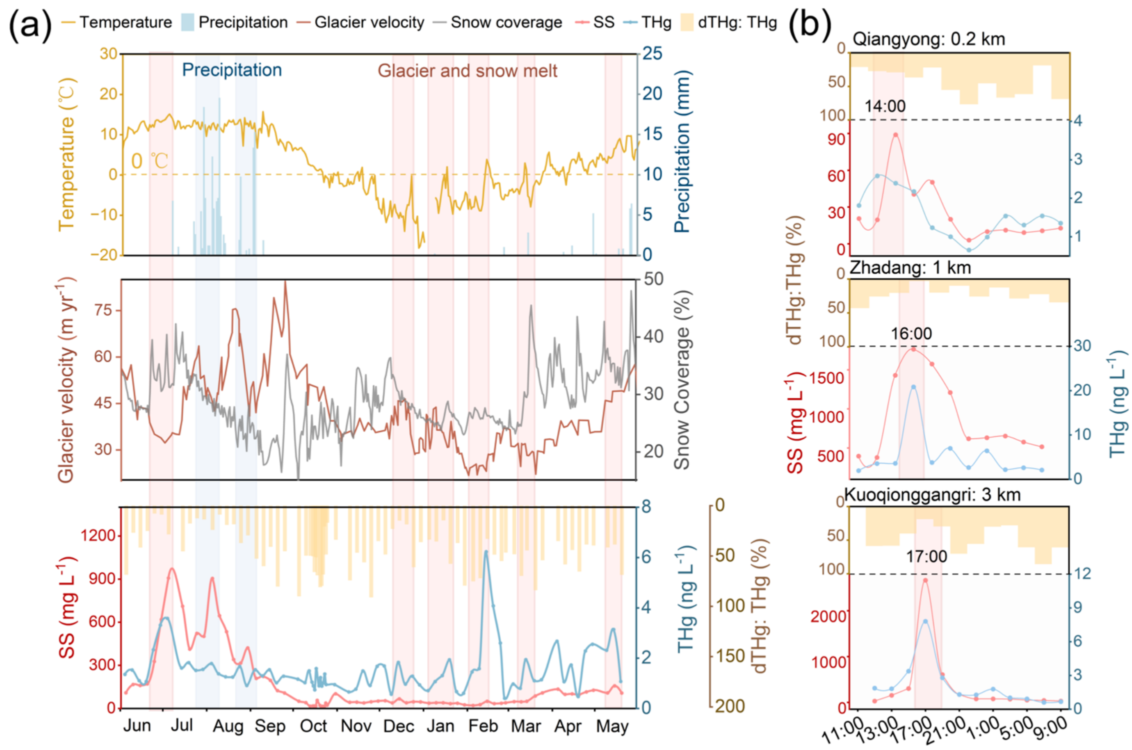

Figure 3. Seasonal and diurnal dynamics of SS and THg in Tibetan Plateau GFSs. (a) Seasonal changes among glacier dynamics, meteorological conditions, and stream SS, THg, and dTHg:THg in the Rongbuk GFS, based on monthly data from June 2019 to May 2020. (b) Diurnal cycles of SS, THg, and dTHg: THg across GFSs, showing afternoon peaks in SS and THg and corresponding minima in dTHg:THg, with peak timing becoming progressively later at sites farther from glacier termini.

tinental catchments: Zhadang (n = 30), Qiangyong (n = 82), and Kuoqionggangri (n = 36). These sites were located approximately 0.1−3 km from glacier termini. Comparisons among the six catchments were restricted to June-September to minimize confounding seasonal hydrological differences.

For each sampling event, duplicate 250 mL fluorinated high-density polyethylene (FLPE) bottles were used to collect Hg and SS. Surface water was collected in the flow direction to avoid resuspension of bottom sediments. Samples for THg were immediately acidified with 0.5% (v/v) double-distilled hydrochloric acid (HCl, BV−III grade, MOS) to minimize adsorption and transformation during transport. dTHg was measured in samples filtered through 0.45 μm membranes (Durapore, Millipore, 47 mm), with the filtrates also preserved to 0.5% HCl. Because the particulate mass retained on individual filters was insufficient for most commonly used direct Hg analysis methods, particulate Hg was not measured directly on suspended particles. Instead, consistent with a common operational approach in the Hg literature, particulate Hg was calculated from paired unfiltered and filtered samples as pTHg = THg − dTHg.[31,32] In this study, we use dTHg: THg as the primary indicator of Hg partitioning between dissolved and particulate phases, with lower dTHg: THg values indicating a greater particulate contribution to the Hg load.

THg and dTHg were quantified by cold vapor atomic fluorescence spectrometry (CVAFS) following USEPA Method 1631. Samples were oxidized with 125 μL bromine monochloride (BrCl) solution to convert all Hg species to Hg^{2+} for 24 h, after which excess oxidant was removed by 50 μL of hydroxylamine hydrochloride. Hg^{2+} was then reduced to elemental Hg^0 using stannous chloride ($SnCl_2$) solution. Pretreated samples were analyzed with a Tekran 2600 Hg analyzer. The method detection limit (MDL) was 0.05 ng L^{-1}, and field and laboratory blanks, which accounted for 10% of all samples, were below 0.01 ng L^{-1}. Additional QA/QC procedures are provided in Text S1.

SS concentrations were determined gravimetrically from the mass difference of filter membranes before and after filtration. After filtration, membranes were dried to constant mass and reweighted. SS concentrations are expressed in mg L^{-1} and calculated by dividing the mass difference by the volume of filtered water.

Other Environmental Data

Meteorological variables, including air temperature and precipitation, were obtained from the Spatially Extensive Long-Term Quality-Assured Land−Atmosphere Interactions Data set over the Tibetan Plateau.[33] Daily fractional snow cover data were derived from the MODIS Daily Cloud-Free Fractional Snow Cover Data set of the Asian Water Tower Region (2000−2022).[34] Glacier surface velocity data were retrieved from the ITSLive Dashboard as a basin-scale indicator of glacier dynamics and erosion potential. Glacier coverage and river discharge were obtained from the Glacier Mass Balance and Meltwater Runoff Simulation and Projection Data set for High Mountain Asia.[35] Glacier coverage (%) was calculated from glacierized area divided by total catchment area, and used to represent glacier influence at the catchment scale, as it integrates ice volume, glacier dynamics, and sediment generation potential.[36−38] Catchment-scale lithological information was compiled from digital geological maps provided by the China Geology Survey Center. Basin-averaged lithology erodibility was derived from the Glim data set of global lithologic distributions and expressed as an erodibility index.[39]

■ RESULTS AND DISCUSSION

Concentration and Spatial Variability in SS and Hg

SS concentrations vary widely among the studied GFSs, with a mean concentration of 400 ± 100 mg L^{-1}; THg concentrations range from 1 to 27 ng L^{-1}, with a mean of 7 ± 3 ng L^{-1}. Overall, THg concentrations in Tibetan Plateau GFSs are comparable to those in Alaska and Arctic Canada, higher than those in several other GFSs with similar glacier coverage (Figure 2a), but lower than those reported for some GFSs in the Andes and South Asia, where contributing catchments are influenced by anthropogenic activities or high bedrock values

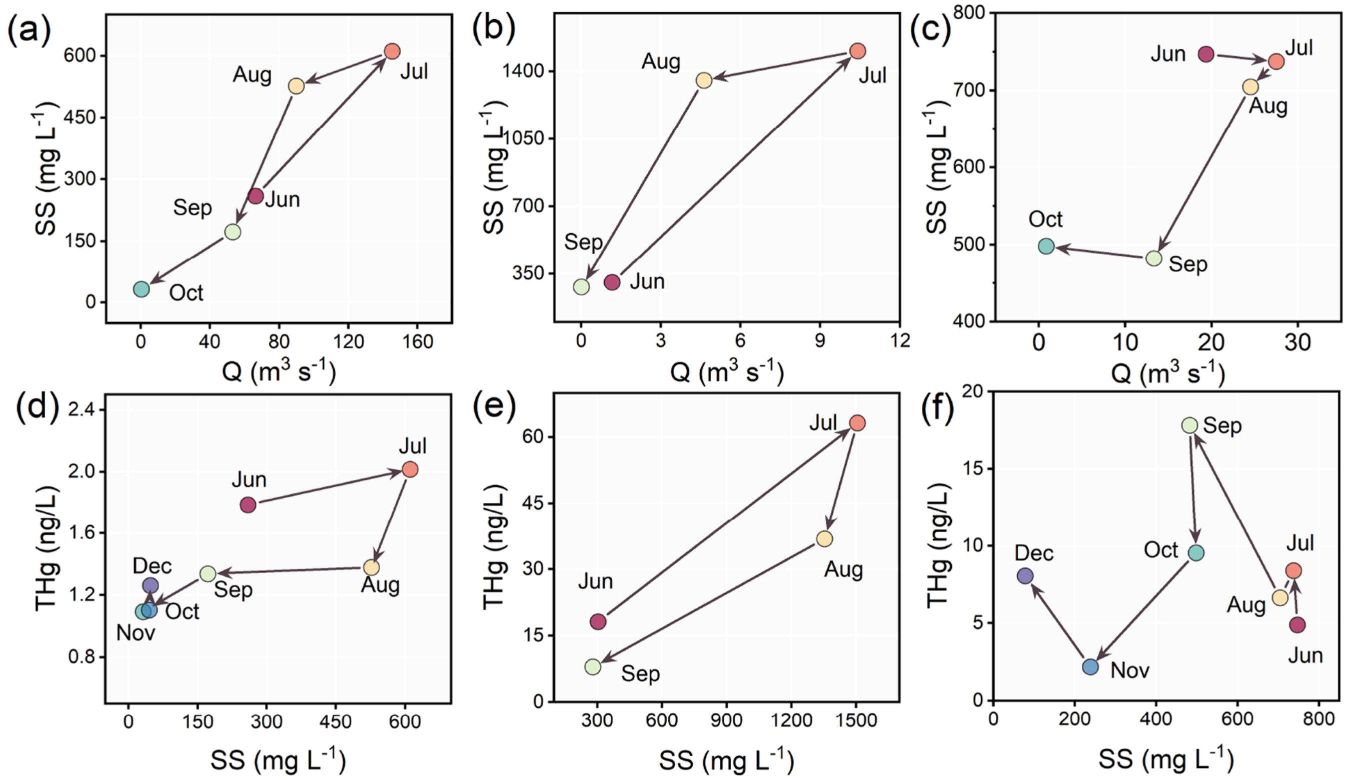

Figure 4. Seasonal hysteresis between discharge (Q), SS, and THg in GFSs with contrasting glacier thermal regimes. (a−c) Monthly hysteresis loops between SS concentration and Q for the Rongbuk (polythermal/subcontinental), Laohugou (cold-based/continental), and Hailuogou (temperate) catchments, respectively. (d−f) Monthly hysteresis loops between THg and SS for the same three catchments.

(Figure S1a).[40,41] THg yields in Tibetan Plateau GFSs average 9 ± 3 g km^{-2} yr^{-1}, similar to values reported for Alaska,[42] but higher than those for Arctic Canada under similar glacier coverage (Figure S1b),[27] large Arctic rivers such as the Yukon and Mackenzie,[43] and Himalaya basins such as the upper Ganges.[44] These comparisons suggest that GFSs on the Tibetan Plateau can mobilize appreciable Hg even in regions without anthropogenic sources.

SS and THg exhibit coherent cross-catchment variability, with higher THg generally occurring in streams with higher SS concentrations (Figure 2b). Laohugou shows the highest SS and THg concentrations, followed by Hailuogou, Zhadang, and the other GFSs. This pattern indicates strong sediment-mediated THg export. Glacier coverage emerges as an important control on spatial SS-THg variability. Catchments with higher glacier coverage generally show elevated SS and THg concentrations, and this relationship becomes clearer when additional published data from Tibetan Plateau GFSs are included (R^2 = 0.77, p < 0.01, Figure 2c). This pattern suggests that glacier extent is an important control on Hg export through its influence on suspended sediment production and transport.[18] The approximately linear SS−THg relationships within individual catchments and the significant covariation between calculated pTHg and THg provide additional support for this interpretation (Figures S2 and S3).

Catchments influenced by upstream proglacial lakes, including Rongbuk and Qiangyong, deviate from this trend. Despite relatively high glacier coverage, GFSs that flow through proglacial lakes show significantly (p < 0.05) lower SS and THg concentrations than other GFSs with comparable glacier coverage (Figure 2a). Similar reductions in Hg yields have also been reported for GFSs with upstream proglacial lakes globally (Figure S1b,c). This pattern is explained by proglacial lakes acting as sedimentation traps that preferentially retain SS and associated Hg during water transit.[45,46] By attenuating particle export, these lakes reduce downstream THg concentrations and weaken the influence of the glacier coverage on Hg export.

Variation in dTHg:THg provides additional insight into Hg partitioning among catchments. Lower dTHg: THg values correspond to a greater particulate contribution,[32] consistent with the higher SS and THg concentrations observed in the studied GFSs (Figure 2b) and further supporting sediment-mediated Hg transport. By contrast, higher dTHg:THg values in lake-influenced catchments most likely reflect preferential removal of suspended particles.[47] In addition, reduced flow velocity and longer water residence times within proglacial lakes may enhance particle−dissolved phase exchange, helping sustain dissolved Hg downstream.[46,48]

Seasonal and Diurnal SS and THg Fluctuations

Across all GFSs, SS and THg concentrations increase during the monsoon season, accompanied by lower dTHg:THg, coincident with periods of intensified meltwater production, rainfall, and glacier motion (Figures 3a, S4, and S5). In the Rongbuk GFS, synchronous increases in SS and THg and decreases in dTHg:THg during periods of rising temperature and declining snow cover are consistent with melt-driven mobilization of particle-associated Hg. However, during intense rainfall events, SS increases disproportionately relative to THg concentration, indicating that rainfall mobilizes additional sediment sources that are less Hg-enriched than subglacially eroded material.[42]

https://doi.org/10.1021/acs.est.6c01369
Environ. Sci. Technol. 2026, 60, 14150−14160

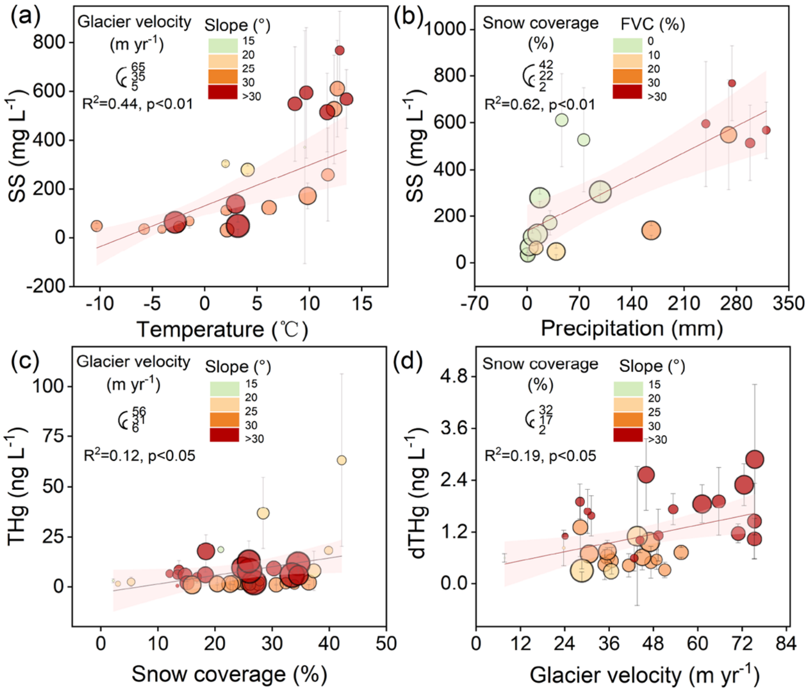

Figure 5. Basin-scale relationships between SS, Hg, and environmental drivers in Tibetan Plateau GFSs, based on monthly averaged basin-scale values to identify broad controls. (a) SS versus air temperature, with basin slope shown by color and glacier velocity by symbol size. (b) SS versus precipitation, with snow coverage shown by color and fractional vegetation cover (FVC) by symbol size. (c) THg versus snow coverage, with basin slope shown by color and glacier velocity by symbol size. (d) dTHg versus glacier velocity, with basin slope shown by color and snow coverage by symbol size. Lines show best-fit linear regressions with 95% confidence intervals; corresponding R^2 and p values are indicated in panels.

Sampling at 2 h intervals reveals pronounced diurnal cycles in SS and THg, with concentrations typically peaking in the afternoon (14:00−17:00), consistent with daily discharge maxima driven by glacier meltwater production.[49] Peak timing becomes progressively later with increasing distance from the glacier terminus. For example, peaks occur earlier at Qiangyong, located ∼0.2 km from the terminus, than at Zhadang and Kuoqionggangri, located ∼1 and ∼3 km from their glacier termini, respectively (Figure 3b), indicating increasing travel time lags along the glacier-proglacial flow paths. This spatial progression suggests that meltwater, sediment, and associated Hg are transferred downstream over hourly time scales, and that temporary storage and delayed transport within the glacier-proglacial system influence the timing of export signals.[50]

Correlation between SS and THg

Across the Tibetan Plateau GFSs, THg concentrations increase with SS concentrations following a log−linear scaling relationship (Figure 2d), consistent with sediment-mediated Hg export from glacierized catchments. This relationship closely matches a global riverine relationship ($\log \text{THg} = 0.42 \times \log \text{SS} + 0.22$, $R^2 = 0.40$, $p < 0.001$),[51] supporting the use of SS as a practical proxy for estimating Hg concentrations and fluxes in data-scarce glacierized catchments. Although individual catchments show approximately linear SS−THg relationships (Figure S2), catchment-specific slopes and intercepts differ, producing a nonlinear pattern when the data are pooled regionally. This likely reflects basin-to-basin differences in particle composition and Hg mineral affinity. Normalizing THg by SS further highlights spatial heterogeneity in THg:SS, with higher values in Laohugou, Hailuogou, and Qiangyong, and lower values in Rongbuk, Kuoqionggangri, and Zhadang (Figure 2e). Catchments with elevated THg:SS are underlain mainly by sedimentary and volcaniclastic lithologies (Table S1), which likely contain higher natural Hg than granitoid-dominate terrains.[52] Together with their higher mean erodibility indices (1.6 ± 0.2 vs 1.1 ± 0.1), this suggests that bedrock lithology and erosion potential both contribute to enhanced sediment production and particle-normalized Hg enrichment.

To assess how sediment supply and routing influence the timing of particle export, we examine hysteresis between SS concentration and discharge (Q), a common indicator of time-varying sediment availability, storage, and transport pathways.[53,54] SS−Q hysteresis patterns differ among glacier thermal regimes (Figure 4a−c) and are consistent with contrasts in subglacial drainage evolution and sediment accessibility. Cold-based and polythermal glaciers, represented by Laohugou and Rongbuk, respectively, display counterclockwise SS−Q hysteresis, with SS lagging behind Q, whereas the temperate Hailuogou Glacier shows clockwise hysteresis, characterized by higher SS on the rising limb of Q followed by a midseason decline. These patterns likely reflect thermal-regime-dependent differences in drainage efficiency and sediment access:[55−58] less efficient drainage in colder systems delays sediment evacuation,[59,60] whereas more efficient early season drainage in temperate systems rapidly mobilizes stored sediment, followed by short-term depletion.[61−63]

Against this sediment transport backdrop, THg-SS hysteresis also differs among glacier types (Figure4 d−f), indicating that Hg enrichment can be temporally offset from sediment export. In cold-based and polythermal systems, represented by Rongbuk and Laohugou, THg peaks precede SS at seasonal scales, a pattern also evident in daily records from Zhadang, Kuoqionggangri, and Qiangyong (Figure S6). In contrast, THg

https://doi.org/10.1021/acs.est.6c01369
Environ. Sci. Technol. 2026, 60, 14150−14160

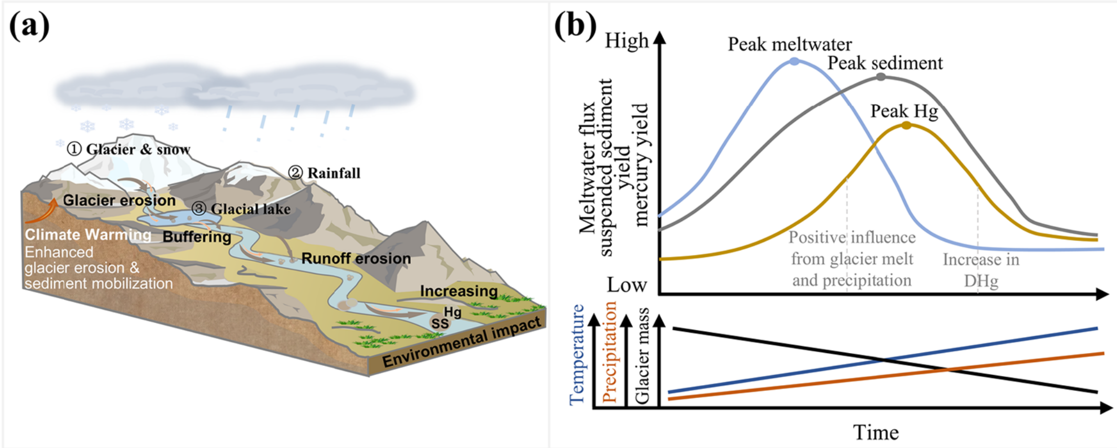

Figure 6. Conceptual framework for controls on SS and Hg export from glacierized catchments and their potential responses to warming. (a) Schematic summary of main processes inferred from this study. (b) Conceptual trajectories illustrating possible shifts in the relative timing of peak meltwater discharge, SS export, and THg export as temperature and precipitation increase and glacier mass delines.

peaks lag behind SS in the temperate Hailuogou Glacier. One possible explanation is that early season melt with low water energy in colder systems preferentially mobilizes Hg-enriched particle fractions, whereas later-season increases in total sediment export dilute THg, consistent with the preferential association of Hg with fine particles of higher surface area.[64,65] In temperate glacier systems, by contrast, efficient early season drainage may rapidly export large sediment loads, while sustained melt later in the season mobilizes newly generated or compositionally distinct particle fractions that continue to support THg export.[66−68]

Factors Controlling the Export of SS and Hg

SS increases with the air temperature and precipitation, consistent with enhanced meltwater production and rainfall-driven sediment mobilization (Figure 5a,b). At the monthly basin scale, precipitation is positively correlated with SS (Figure S7; $p < 0.05$) but shows no significant relationship with THg concentration, indicating that rainfall enhances SS export more than it increases THg concentration. This decoupling between SS and THg suggests that rainfall-driven increases in sediment export do not appear to involve proportional increases in Hg enrichment and may reflect either mobilization of relatively low-Hg sediment sources from proglacial areas or particle sorting that alters the composition of exported material.[69,70]

THg shows weak but significant ($p < 0.05$) positive associations with snow coverage and glacier velocity (Figure 5c), and a broader global compilation similarly suggests that catchments with faster glacier velocities tend to have higher THg concentrations (Figure S8). Together with glacier coverage and basin slope, glacier velocity reflects basin-scale glacier influence and erosion potential rather than event-scale forcing. These patterns suggest that catchments with stronger glacier influence and greater erosional potential tend to export more Hg.[71] The dissolved fraction also shows a weak positive but significant ($p < 0.05$) association with glacier velocity (Figure 5d), possibly reflecting enhanced mineral-water interactions and particle−water exchange along subglacial and proglacial flow paths.[72]

Using reported ice core Hg concentrations of ∼1 ng L^{-1},[73,74] snow pit Hg concentrations (Table S3), and published estimates of glacier volume and glacier mass loss rates on the Tibetan Plateau,[23,35] we estimate a total Tibetan Plateau THg reservoir of ∼18 Mg, and an ice melt THg release of ∼0.06 Mg yr^{-1}. These first-order estimates are uncertain because they assume that available ice core and snow-pit Hg concentrations are regionally representative, and that published glacier volume and mass loss data adequately represent plateau-scale glacier storage and meltwater release. Observed THg concentrations in Tibetan Plateau GFSs (7 ± 3 ng L^{-1} in this study) are much higher than published ice core values, implying contributions beyond direct ice melt, most plausibly from subglacial-derived Hg. Upscaling observed THg concentrations using published glacial runoff estimates[35] suggests basin-integrated THg exports of ∼0.7 Mg yr^{-1}, more than an order of magnitude greater than the ice melt estimate. Despite the uncertainty, the mismatch supports the inference that erosion-driven Hg export dominates over Hg release from direct ice melt release at the regional scale.

Future Climate Change Impacts on Hg Cycling

Our observations identify three climate-sensitive factors likely to influence Hg export from glacierized catchments: glacial meltwater production, rainfall events, and the formation of proglacial lakes (Figure 6A). Across the Tibetan Plateau GFSs, the positive covariation among SS, THg, glacier coverage, glacier velocity, and catchment slope supports a strong particulate pathway for Hg mobilization linked to glacial erosion and downstream sediment transport. Under continued warming, increased meltwater flux may enhance sediment production,[18,71] and contribute to particle-associated Hg export.[37,75] Rainfall may further drive event-driven sediment mobilization but with asymmetric responses between SS and THg. Rainfall leads to higher SS concentrations, yet it shows a weak positive influence on THg concentration (Figure S7), indicating that SS responds more strongly and rapidly to rainfall than THg. As a result, rainfall can increase Hg export primarily through enhanced runoff and sediment flux rather than proportional increases in THg concentrations. In addition, a shift from snowfall to rainfall over glacier surfaces may enhance water delivery to glacier beds, strengthen subglacial drainage, and further promote glacial erosion and particle-associated Hg mobilization.[76,77]

Proglacial lakes are associated with lower SS and THg yields and higher dissolved fractions, indicating that they buffer

https://doi.org/10.1021/acs.est.6c01369
Environ. Sci. Technol. 2026, 60, 14150−14160

downstream Hg export by preferentially trapping SS- and particle-bound Hg. As glacier retreat promotes lake formation and expansion, downstream Hg export may temporarily decouple from upstream sediment production, while the dissolved fraction may contribute a larger share under longer residence times and altered hydrological connectivity.[45,78] At the same time, episodic lake outbursts could remobilize Hg pools and may generate pulses of sediment and Hg, increasing the temporal variability of Hg delivery from glacierized headwaters.[79,80]

Previous studies suggest that climate warming can initially increase glacial sediment yields until a maximum ("peak sediment") is reached, followed by a decline, with this transition typically lagging behind peak meltwater discharge.[81] Building on this framework and on the particulate dominance observed in our data, our results suggest that peak Hg export may occur later than peak sediment export because Hg export depends not only on sediment quantity but also on particle Hg content and Hg partitioning between dissolved and particulate phases. Early in glacier retreat, high meltwater discharge and strong mechanical erosion may maximize SS export, whereas Hg export may not peak concurrently if the exported material is dominated by coarser, less Hg-enriched fractions. As glacial retreat progresses, shifts in sediment sources, particle sorting, and hydrological routing may favor the preferential transport of finer and more Hg-enriched fine particles, allowing THg export to remain elevated even as bulk sediment yields decline. At the same time, expanding proglacial lakes and longer residence times may shift Hg partitioning toward a greater dissolved contribution. Together, these processes provide a plausible mechanistic basis for delayed "peak Hg" export relative to "peak sediment" (Figure 6b), although the magnitude and timing of this offset likely vary among basins.

Main Findings and Implications

Glacier coverage and glacier dynamics emerge as major controls on THg concentrations and yields across the Tibetan Plateau GFSs. Hg export is strongly sediment-mediated, and Tibetan Plateau GFSs show relatively high THg concentration and yields compared with many other GFSs with comparable glacier coverage, consistent with the high SS yields of this region.[18] Precipitation enhances SS more strongly than THg concentration, suggesting that rainfall increases Hg export through increased runoff and sediment flux, but that the particles mobilized are comparatively Hg-deplete compared to those mobilized by glaciers.[18,82] Proglacial lakes reduce downstream SS and THg export, highlighting their role as buffers of particulate Hg transport and as an additional source of variability in downstream Hg export, especially under potential glacial lake outbursts.[83,84] Continued glacier retreat is likely to alter both the magnitude and timing of Hg export from high mountain headwaters, including the possibility that peak THg export may lag peak sediment export.

Besides, higher dissolved fractions in lake-influenced basins indicate that proglacial lakes act not only as buffers of particulate Hg export but also as modifiers of Hg partitioning during transport. Glaicer melt has been reported to release bioavailable organic matter.[85] Proglacial lakes and other depositional zones may therefore provide more favorable conditions for downstream Hg processing because of longer water residence times, enhanced particle−water exchange, and greater biogeochemical activity.[86,87] Previous studies have also suggested that such settings can support enhanced Hg transformation potential.[88] Although MeHg was not tested, thus specific transformation pathways were not examined in this study, we suggest a potential shift in downstream Hg biogeochemistry under continued glacier retreat.[89,90]

These findings suggest that climate-driven glacier retreat may enhance Hg export from high mountain headwaters with implications for downstream water quality and ecosystem exposure. This glacier-associated Hg pathway and its downstream implications are not explicitly considered in the IPCC Sixth Assessment reports, highlighting the need to incorporate it into future climate-water quality risk assessments and policy frameworks, particularly in regions that rely on glacier-fed water resources.

■ ASSOCIATED CONTENT

Supporting Information

The Supporting Information is available free of charge at https://pubs.acs.org/doi/10.1021/acs.est.6c01369.

Quality assurance and quality control on Hg measurements (Text S1) and published Hg data in GFSs and snow pits (PDF)

■ AUTHOR INFORMATION

Corresponding Author

Dongfeng Li − *Key Laboratory for Water and Sediment Sciences, Ministry of Education, College of Environmental Sciences and Engineering, Peking University, Beijing 100871, China; State Key Laboratory of Plateau Ecology and Agriculture, Qinghai University, Xining 810016, China*; Email: dongfeng.li@pku.edu.cn

Authors

Mingyue Li − *Key Laboratory for Water and Sediment Sciences, Ministry of Education, College of Environmental Sciences and Engineering, Peking University, Beijing 100871, China; State Key Laboratory of Tibetan Plateau Earth System, Environment and Resources (TPESER), Institute of Tibetan Plateau Research, Chinese Academy of Sciences, Beijing 100101, China*; orcid.org/0009-0006-5578-5468

Xuejun Sun − *School of Environment and Resources, Shanxi University, Taiyuan 030000, China*

Jon R. Hawkings − *Department of Earth and Environmental Science, University of Pennsylvania, Philadelphia, Pennsylvania 19104, United States*

Jeroen E. Sonke − *Géosciences Environnement Toulouse, CNRS, IRD, Université Toulouse, 31062 Toulouse, France*; orcid.org/0000-0001-7146-3035

Yanxu Zhang − *Department of Earth and Environmental Sciences, Tulane University, New Orleans, Louisiana 70118, United States*

Qianggong Zhang − *State Key Laboratory of Tibetan Plateau Earth System, Environment and Resources (TPESER), Institute of Tibetan Plateau Research, Chinese Academy of Sciences, Beijing 100101, China; International Centre for Integrated Mountain Development, Kathmandu 44700, Nepal; University of Chinese Academy of Sciences, Beijing 100049, China*; orcid.org/0000-0002-2189-4248

Complete contact information is available at: https://pubs.acs.org/10.1021/acs.est.6c01369

https://doi.org/10.1021/acs.est.6c01369
Environ. Sci. Technol. 2026, 60, 14150−14160

Notes

The authors declare no competing financial interest.

■ ACKNOWLEDGMENTS

This study was supported by the Fundamental and Interdisciplinary Disciplines Breakthrough Plan of the Ministry of Education of China (JYB2025XDXM910), the National Natural Science Foundation of China (NSFC Grant No. 52479055), the Excellent Young Scientists Fund of the NSFC, and the State Key Laboratory of Plateau Ecology and Agriculture, Qinghai University (2025-ZJ-J09). Q.Z. acknowledges support from the National Natural Science Foundation of China (42022003). M.L. acknowledges the China Postdoctoral Science Foundation (2025M780293) and PKU Boya Postdoctoral Fellowship.

■ REFERENCES

(1) Poulin, B. A.; Tate, M. T.; Janssen, S. E.; Aiken, G. R.; Krabbenhoft, D. P. A comprehensive sulfate and DOM framework to assess methylmercury formation and risk in subtropical wetlands. *Nat. Commun.* **2025**, *16* (1), No. 4253.

(2) Fritz, B.; Peregovich, B.; Tenório, L. D.; Alves, A. C. D.; Schmidt, M. Mercury and CO2 emissions from artisanal gold mining in Brazilian Amazon rainforest. *Nat. Sustainability* **2024**, *7* (1), 15−22.

(3) Peng, D.; Tan, Z.; Yuan, T.; Wu, P.; Song, Z.; Zhang, P.; Huang, S.; Zhang, Y.; Lei, T.; Middleton, B. A.; Sonke, J. E.; Lei, G.; Gao, J. Human perturbations to mercury in global rivers. *Sci. Adv.* **2025**, *11* (24), 7614−7620.

(4) Feinberg, A.; Selin, N. E.; Braban, C. F.; Chang, K. L.; Custódio, D.; Jaffe, D. A.; Kyllönen, K.; Landis, M. S.; Leeson, S. R.; Luke, W.; Molepo, K. M.; Murovec, M.; Mastromonaco, M. G. N.; Pfaffhuber, K. A.; Rüdiger, J.; Sheu, G. R.; St Louis, V. L. Unexpected anthropogenic emission decreases explain recent atmospheric mercury concentration declines. *Proc. Natl. Acad. Sci. U.S.A.* **2024**, *121* (42), No. e2401950121.

(5) Faïn, X.; Ferrari, C. P.; Dommergue, A.; Albert, M. R.; Battle, M.; Severinghaus, J.; Arnaud, L.; Barnola, J. M.; Cairns, W.; Barbante, C.; Boutron, C. Polar firn air reveals large-scale impact of anthropogenic mercury emissions during the 1970s. *Proc. Natl. Acad. Sci. U.S.A.* **2009**, *106* (38), 16114−16119.

(6) Schaefer, K.; Elshorbany, Y.; Jafarov, E.; Schuster, P. F.; Striegl, R. G.; Wickland, K. P.; Sunderland, E. M. Potential impacts of mercury released from thawing permafrost. *Nat. Commun.* **2020**, *11* (1), No. 4650.

(7) Feng, X. B.; Wang, X.; Jia, L. Y.; Yuan, W.; Lu, M.; Liu, N. T.; Wu, F.; Cai, X. Y.; Wang, F. Y.; Lin, C. J. Influence of global warming and human activity on mercury accumulation patterns in wetlands across the Qinghai-Tibet Plateau. *Natl. Sci. Rev.* **2025**, *12* (1), No. nwae414.

(8) McConnell, J. R.; Edwards, R. Coal burning leaves toxic heavy metal legacy in the Arctic. *Proc. Natl. Acad. Sci. U.S.A.* **2008**, *105* (34), 12140−12144.

(9) Zhou, C. Z.; Liu, M. D.; Mason, R. P.; Assavapanuvat, P.; Zhang, N. H.; Bianchi, T. S.; Zhang, Q. R.; Li, X. L.; Sun, R. Y.; Chen, J. B.; Wang, X. J.; Raymond, P. A. Warming-induced retreat of West Antarctic glaciers weakened carbon sequestration ability but increased mercury enrichment. *Nat. Commun.* **2025**, *16* (1), No. 1831.

(10) Huang, J.; Kang, S.; Liu, J.; Tang, W.; Guo, J.; Zhang, Q.; Tripathee, L.; Zhang, Y.; Wang, F. Glaciers in Western China as a significant global pool of cryospheric methylmercury. *Sci. Bull.* **2026**, *71* (3), 525−529.

(11) Kang, S.; Wang, F.; Morgenstern, U.; Zhang, Y.; Grigholm, B.; Kaspari, S.; Schwikowski, M.; Ren, J.; Yao, T.; Qin, D.; Mayewski, P. A. Dramatic loss of glacier accumulation area on the Tibetan Plateau revealed by ice core tritium and mercury records. *Cryosphere* **2015**, *9* (3), 1213−1222.

(12) Dastoor, A.; Angot, H.; Bieser, J.; Christensen, J. H.; Douglas, T. A.; Heimburger-Boavida, L.-E.; Jiskra, M.; Mason, R. P.; McLagan, D. S.; Obrist, D.; Outridge, P. M.; Petrova, M. V.; Ryjkov, A.; Pierre, K. A. S.; Schartup, A. T.; Soerensen, A. L.; Toyota, K.; Travnikov, O.; Wilson, S. J.; Zdanowicz, C. Arctic mercury cycling. *Nat. Rev. Earth Environ.* **2022**, *3* (4), 270−286.

(13) Delaney, I.; Lardet, F.; Jenkin, M.; Mancini, D.; Lane, S. N. Different geomorphic processes control suspended sediment and bedload export from glaciers. *Nat. Commun.* **2025**, *16* (1), No. 6005.

(14) Li, X.; Wang, N.; Ding, Y.; Hawkings, J. R.; Yde, J. C.; Raiswell, R.; Liu, J.; Zhang, S.; Kang, S.; Wang, R.; Liu, Q.; Liu, S.; Bol, R.; You, X.; Li, G. Globally elevated chemical weathering rates beneath glaciers. *Nat. Commun.* **2022**, *13* (1), No. 407.

(15) Zhang, Q.; Zhang, F.; Kang, S.; Cong, Z. Melting glaciers: Hidden hazards. *Science* **2017**, *356* (6337), 495.

(16) Xue, Y. L.; Tu, X. H.; Nie, Y. G.; Wu, L. B.; Zhang, H. J.; Wang, Z. Y.; Su, G. S.; Liu, X. D. Secondary releases of legacy heavy metals to proglacial ecosystems from melting Arctic glaciers. *J. Hazard. Mater.* **2025**, *496*, No. 139290.

(17) Liu, N.; Li, X.; Chen, P.; Yuan, W.; Lin, C.-J.; Feng, X.; Wang, X. Mercury Transport, Transformation and Accumulation Recorded by Stable Isotopes during Retreated Glacier Chronosequence of 250 Years. *Environ. Sci. Technol.* **2025**, *59* (12), 6085−6096.

(18) Li, D.; Zhang, T.; Walling, D. E.; Lane, S.; Bookhagen, B.; Tian, S.; Overeem, I.; Syvitski, J.; Kettner, A. J.; Park, E.; Koppes, M.; Schmitt, R. J. P.; Sun, W.; Ni, J.; Ehlers, T. A. The competing controls of glaciers, precipitation, and vegetation on high-mountain fluvial sediment yields. *Sci. Adv.* **2024**, *10* (48), No. eads6196.

(19) Hawkings, J. R.; Linhoff, B. S.; Wadham, J. L.; Stibal, M.; Lamborg, C. H.; Carling, G. T.; Lamarche-Gagnon, G.; Kohler, T. J.; Ward, R.; Hendry, K. R.; Falteisek, L.; Kellerman, A. M.; Cameron, K. A.; Hatton, J. E.; Tingey, S.; Holt, A. D.; Vinsova, P.; Hofer, S.; Bulinova, M.; Vetrovsky, T.; Meire, L.; Spencer, R. G. M. Large subglacial source of mercury from the southwestern margin of the Greenland Ice Sheet. *Nat. Geosci.* **2021**, *14* (7), 496−513.

(20) Miller, H. R.; Driscoll, C. T.; Janssen, S. E.; Hinckley, E.-L. S. Climate-driven sulfate export in alpine watersheds may stimulate methylmercury production. *Environ. Res. Lett.* **2025**, *20* (6), No. 064049.

(21) Jonsson, S.; Andersson, A.; Nilsson, M. B.; Skyllberg, U.; Lundberg, E.; Schaefer, J. K.; Akerblom, S.; Bjorn, E. Terrestrial discharges mediate trophic shifts and enhance methylmercury accumulation in estuarine biota. *Sci. Adv.* **2017**, *3* (1), No. e1601239.

(22) Staniszewska, K. J.; Reyes, A. V.; Cooke, C. A. Glacial erosion drives high summer mercury exports from the Yukon River, Canada. *Environ. Sci. Technol. Lett.* **2023**, *10* (11), 1117−1124.

(23) Yao, T.; Bolch, T.; Chen, D.; Gao, J.; Immerzeel, W.; Piao, S.; Su, F.; Thompson, L.; Wada, Y.; Wang, L.; Wang, T.; Wu, G.; Xu, B.; Yang, W.; Zhang, G.; Zhao, P. The imbalance of the Asian water tower. *Nat. Rev. Earth Environ.* **2022**, *3* (10), 618−632.

(24) Hugonnet, R.; McNabb, R.; Berthier, E.; Menounos, B.; Nuth, C.; Girod, L.; Farinotti, D.; Huss, M.; Dussaillant, I.; Brun, F.; Kaab, A. Accelerated global glacier mass loss in the early twenty-first century. *Nature* **2021**, *592* (7856), 726−731.

(25) Immerzeel, W. W.; van Beek, L. P. H.; Bierkens, M. F. P. Climate Change Will Affect the Asian Water Towers. *Science* **2010**, *328* (5984), 1382−1385.

(26) Zolkos, S.; Zhulidov, A. V.; Gurtovaya, T. Y.; Gordeev, V. V.; Berdnikov, S.; Pavlova, N.; Kalko, E. A.; Kuklina, Y. A.; Zhulidov, D. A.; Kosmenko, L. S.; Shiklomanov, A. I.; Suslova, A.; Geyman, B. M.; Thackray, C. P.; Sunderland, E. M.; Tank, S. E.; McClelland, J. W.; Spencer, R. G. M.; Krabbenhoft, D. P.; Robarts, R.; Holmes, R. M. Multidecadal declines in particulate mercury and sediment export from Russian rivers in the pan-Arctic basin. *Proc. Natl. Acad. Sci. U.S.A.* **2022**, *119* (14), No. e2119857119.

(27) St Pierre, K. A.; Louis, V. L. S.; Lehnherr, I.; Gardner, A. S.; Serbu, J. A.; Mortimer, C. A.; Muir, D. C. G.; Wiklund, J. A.; Lemire, D.; Szostek, L.; Talbot, C. Drivers of mercury cycling in the rapidly changing glacierized watershed of the High Arctic's largest lake by

Volume (Lake Hazen, Nunavut, Canada). *Environ. Sci. Technol.* **2019**, *53* (3), 1175−1185.
(28) Li, D. F.; Lu, X. X.; Overeem, I.; Walling, D. E.; Syvitski, J.; Kettner, A. J.; Bookhagen, B.; Zhou, Y. J.; Zhang, T. Exceptional increases in fluvial sediment fluxes in a warmer and wetter High Mountain Asia. *Science* **2021**, *374* (6567), 599−603.
(29) Shi, Y. F.; Liu, S. Y. Estimation on the response of glaciers in China to the global warming in the 21st century. *Chin. Sci. Bull.* **2000**, *45* (7), 668−672.
(30) Yao, T.; Thompson, L.; Yang, W.; Yu, W.; Gao, Y.; Guo, X.; Yang, X.; Duan, K.; Zhao, H.; Xu, B.; Pu, J.; Lu, A.; Xiang, Y.; Kattel, D. B.; Joswiak, D. Different glacier status with atmospheric circulations in Tibetan Plateau and surroundings. *Nat. Clim. Change* **2012**, *2* (9), 663−667.
(31) Sun, X.; Zhang, Q.; Li, M.; Wang, J.; Lu, Z.; Guo, J.; Kang, S.; Shi, J. Insight into the relationships between total suspended particles and mercury in meltwater in a typical glacierized basin in the inland Tibetan Plateau. *J. Hazard. Mater.* **2023**, *452*, No. 131250.
(32) Riscassi, A. L.; Scanlon, T. M. Particulate and dissolved mercury export in streamwater within three mid-Appalachian forested watersheds in the US. *J. Hydrol.* **2013**, *501*, 92−100.
(33) Ma, Y.; Hu, Z.; Xie, Z.; Ma, W.; Wang, B.; Chen, X.; Li, M.; Zhong, L.; Sun, F.; Gu, L.; Han, C.; Zhang, L.; Liu, X.; Ding, Z.; Sun, G.; Wang, S.; Wang, Y.; Wang, Z. A long-term (2005−2016) dataset of hourly integrated land-atmosphere interaction observations on the Tibetan Plateau. *Earth Syst. Sci. Data* **2020**, *12* (4), 2937−2957.
(34) Pan, F.; Jiang, L.; Wang, G.; Pan, J.; Huang, J.; Zhang, C.; Cui, H.; Yang, J.; Zheng, Z.; Wu, S.; Shi, J. MODIS daily cloud-gap-filled fractional snow cover dataset of the Asian Water Tower region (2000−2022). *Earth Syst. Sci. Data* **2024**, *16* (5), 2501−2523.
(35) Zhao, H. Y.; Su, B.; Lei, H. J.; Zhang, T.; Xiao, C. D. A new projection for glacier mass and runoff changes over High Mountain Asia. *Sci. Bull.* **2023**, *68* (1), 43−47.
(36) Herman, F.; De Doncker, F.; Delaney, I.; Prasicek, G.; Koppes, M. The impact of glaciers on mountain erosion. *Nat. Rev. Earth Environ.* **2021**, *2* (6), 422−435.
(37) Koppes, M.; Hallet, B.; Rignot, E.; Mouginot, J.; Wellner, J. S.; Boldt, K. Observed latitudinal variations in erosion as a function of glacier dynamics. *Nature* **2015**, *526* (7571), 100−103.
(38) Dehecq, A.; Gourmelen, N.; Gardner, A. S.; Brun, F.; Goldberg, D.; Nienow, P. W.; Berthier, E.; Vincent, C.; Wagnon, P.; Trouve, E. Twenty-first century glacier slowdown driven by mass loss in High Mountain Asia. *Nat. Geosci.* **2019**, *12* (1), 22−29.
(39) Moosdorf, N.; Cohen, S.; von Hagke, C. A global erodibility index to represent sediment production potential of different rock types. *Appl. Geogr.* **2018**, *101*, 36−44.
(40) Lone, A.; Jeelani, G.; Deshpande, R. D.; Kang, S. C.; Huang, J. Hydrochemical assessment (major ions and Hg) of meltwater in high altitude glacierized Himalayan catchment. *Environ. Monit. Assess.* **2019**, *191* (4), No. 213, DOI: 10.1007/s10661-019-7338-y.
(41) Carpio, A. L. D.; Salcedo, Y. C. Mercury in a high altitude Andes stream with strong impact by artisanal auriffer mining (La Rinconada, Puno, Peru). *Rev. Int. Contam. Ambiental* **2020**, *36* (1), 33−44.
(42) Nagorski, S. A.; Vermilyea, A. W.; Lamborg, C. H. Mercury export from glacierized Alaskan watersheds as influenced by bedrock geology, watershed processes, and atmospheric deposition. *Geochim. Cosmochim. Acta* **2021**, *304*, 32−49.
(43) Zolkos, S.; Krabbenhoft, D. P.; Suslova, A.; Tank, S. E.; McClelland, J. W.; Spencer, R. G. M.; Shiklomanov, A.; Zhulidov, A. V.; Gurtovaya, T.; Zimov, N.; Zimov, S.; Mutter, E. A.; Kutny, L.; Amos, E.; Holmes, R. M. Mercury Export from Arctic Great Rivers. *Environ. Sci. Technol.* **2020**, *54* (7), 4140−4148.
(44) Sun, X.; Zhang, Q.; Li, M.; Kandel, K.; Rawat, B.; Pandey, A.; Guo, J.; Kang, S.; Pant, R. R.; Cong, Z.; Zhang, F. Mercury variation and export in trans-Himalayan rivers: Insights from field observations in the Koshi River. *Sci. Total Environ.* **2020**, *738*, No. 139836.
(45) Sun, X.; Zhang, Q.; Zhang, G.; Li, M.; Li, S.; Guo, J.; Dong, H.; Zhou, Y.; Kang, S.; Wang, X.; Shi, J. Melting Himalayas and mercury export: Results of continuous observations from the Rongbuk Glacier on Mt. Everest and future insights. *Water Res.* **2022**, *218*, No. 118474.
(46) Li, M.; Shi, G.; Li, Y.; Yan, X.; Sun, X.; Yangzong, D.; Li, S.; Dong, H.; Zhou, Y.; Wang, X.; Kang, S.; Zhang, Q. Isotopic Constraints on Sources and Transformations of Nitrate in the Mount Everest Proglacial Water. *Environ. Sci. Technol.* **2023**, *57* (49), 20844−20853.
(47) Selvendiran, P.; Driscoll, C. T.; Montesdeoca, M. R.; Choi, H. D.; Holsen, T. M. Mercury dynamics and transport in two Adirondack lakes. *Limnol. Oceanogr.* **2009**, *54* (2), 413−427.
(48) Canário, J.; Poissant, L.; O'Driscoll, N.; Vale, C.; Pilote, M.; Lean, D. Sediment processes and mercury transport in a frozen freshwater fluvial lake (Lake St. Louis, QC, Canada). *Environ. Pollut.* **2009**, *157* (4), 1294−1300.
(49) Gao, T.; Kang, S.; Zhang, T.; Zhou, S.; Cuo, L.; Sillanpaa, M.; Zhang, Y. Summer hydrological characteristics in glacier and non-glacier catchments in the Nam Co Basin, southern Tibetan Plateau. *Environ. Earth Sci.* **2015**, *74* (3), 2019−2028.
(50) Sun, X. J.; Wang, K.; Kang, S. C.; Guo, J. M.; Zhang, G. S.; Huang, J.; Cong, Z. Y.; Sun, S. W.; Zhang, Q. G. The role of melting alpine glaciers in mercury export and transport: An intensive sampling campaign in the Qugaqie Basin, inland Tibetan Plateau. *Environ. Pollut.* **2017**, *220*, 936−945.
(51) Liu, M. D.; Zhang, Q. R.; Maavara, T.; Liu, S. D.; Wang, X. J.; Raymond, P. A. Rivers as the largest source of mercury to coastal oceans worldwide. *Nat. Geosci.* **2021**, *14* (9), 672−677.
(52) Tian, Z. D.; Lehmann, B.; Deng, C. Z.; Luo, A. B.; Zhang, X. C.; Moynier, F.; Yin, R. S. Mercury abundance and isotopic composition in granitic rocks: Implications for Hg cycling in the upper continental crust. *Geochim. Cosmochim. Acta* **2023**, *361*, 200−209.
(53) Zhang, T.; Li, D.; Kettner, A. J.; Zhou, Y.; Lu, X. Constraining Dynamic Sediment-Discharge Relationships in Cold Environments: The Sediment-Availability-Transport (SAT) Model. *Water Resour. Res.* **2021**, *57* (10), No. e2021WR030690.
(54) Singh, A. T.; Sharma, P.; Sharma, C.; Laluraj, C. M.; Patel, L.; Pratap, B.; Oulkar, S.; Thamban, M. Water discharge and suspended sediment dynamics in the Chandra River, Western Himalaya. *J. Earth Syst. Sci.* **2020**, *129* (1), No. 206.
(55) Comiti, F.; Mao, L.; Penna, D.; Dell'Agnese, A.; Engel, M.; Rathburn, S.; Cavalli, M. Glacier melt runoff controls bedload transport in Alpine catchments. *Earth Planet. Sci. Lett.* **2019**, *520*, 77−86.
(56) Joshi, R.; Khan, A.; Pant, N. C.; Agnihotri, V.; Verma, K.; Kumar, P. Geochemical characteristics and suspended sediments dynamics in the meltwater from the Gangotri Glacier, Garhwal Himalaya, India. *Environ. Earth Sci.* **2023**, *82* (6), No. 150.
(57) Delaney, I.; Adhikari, S. Increased Subglacial Sediment Discharge in a Warming Climate: Consideration of Ice Dynamics, Glacial Erosion, and Fluvial Sediment Transport. *Geophys. Res. Lett.* **2020**, *47* (7), No. e2019GL085672.
(58) Delaney, I.; Bauder, A.; Werder, M. A.; Farinotti, D. Regional and Annual Variability in Subglacial Sediment Transport by Water for Two Glaciers in the Swiss Alps. *Front. Earth Sci.* **2018**, *6*, No. 175.
(59) Guillon, H.; Mugnier, J. L.; Buoncristiani, J. F. Proglacial sediment dynamics from daily to seasonal scales in a glaciated Alpine catchment (Bossons glacier, Mont Blanc massif, France). *Earth Surf. Processes Landforms* **2018**, *43* (7), 1478−1495.
(60) Swift, D. A.; Nienow, P. W.; Spedding, N.; Hoey, T. B. Geomorphic implications of subglacial drainage configuration: rates of basal sediment evacuation controlled by seasonal drainage system evolution. *Sediment. Geol.* **2002**, *149* (1−3), 5−19.
(61) Perolo, P.; Bakker, M.; Gabbud, C.; Moradi, G.; Rennie, C.; Lane, S. N. Subglacial sediment production and snout marginal ice uplift during the late ablation season of a temperate valley glacier. *Earth Surf. Processes Landforms* **2019**, *44* (5), 1117−1136.
(62) Kido, D.; Chikita, K. A.; Hirayama, K. Subglacial drainage system changes of the Gulkana Glacier, Alaska: discharge and

sediment load observations and modelling. *Hydrol. Process.* **2007**, *21* (3), 399−410.
(63) Delaney, I.; Tedstone, A. J.; Werder, M. A.; Farinotti, D. Sediment transport capacity response to variations in water discharge in pressurized subglacial channels. *Cryosphere* **2025**, *19* (8), 2779−2795.
(64) Haritashya, U. K.; Kumar, A.; Singh, P. Particle size characteristics of suspended sediment transported in meltwater from the Gangotri Glacier, central Himalaya - An indicator of subglacial sediment evacuation. *Geomorphology* **2010**, *122* (1−2), 140−152.
(65) Xu, J.; Bland, G. D.; Gu, Y.; Ziaei, H.; Xiao, X. Y.; Deonarine, A.; Reible, D.; Bireta, P.; Hoelen, T. P.; Lowry, G. V. Impacts of Sediment Particle Grain Size and Mercury Speciation on Mercury Bioavailability Potential. *Environ. Sci. Technol.* **2021**, *55* (18), 12393−12402.
(66) Delaney, I.; Anderson, L.; Herman, F. Modeling the spatially distributed nature of subglacial sediment transport and erosion. *Earth Surf. Dyn.* **2023**, *11* (4), 663−680.
(67) Kohler, T. J.; Zársky, J. D.; Yde, J. C.; Lamarche-Gagnon, G.; Hawkings, J. R.; Tedstone, A. J.; Wadham, J. L.; Box, J. E.; Beaton, A. D.; Stibal, M. Carbon dating reveals a seasonal progression in the source of particulate organic carbon exported from the Greenland Ice Sheet. *Geophys. Res. Lett.* **2017**, *44* (12), 6209−6217.
(68) Schillereff, D. N.; Chiverrell, R. C.; Macdonald, N.; Hooke, J. M. Flood stratigraphies in lake sediments: A review. *Earth-Sci. Rev.* **2014**, *135*, 17−37.
(69) Bao, Z. W.; Bain, J.; Holland, S. P.; Wilson, D.; Ptacek, C. J.; Blowes, D. W. Hydrogeochemical Response of a Variably Saturated Sulfide-Bearing Mine Waste-Rock Pile to Precipitation: A Field-Scale Study in the Discontinuous Permafrost Region of Northern Canada. *Water Resour. Res.* **2022**, *58* (1), No. e2021WR031082.
(70) Ku, P. J.; Tsui, M. T. K.; Uzun, H.; Chen, H.; Dahlgren, R. A.; Hoang, T. C.; Karanfil, T.; Zhong, H.; Miao, A. J.; Pan, K.; Coleman, J. S.; Chow, A. T. S. Dominance of Particulate Mercury in Stream Transport and Rapid Watershed Recovery from Wildfires in Northern California, USA. *Environ. Sci. Technol.* **2024**, *58* (50), 22159−22169.
(71) Norris, S. L.; Gosse, J. C.; Millan, R.; Mouginot, J.; Rabatel, A.; Morlighem, M.; Bolton, M. S. M.; Alley, R. B. Drivers of global glacial erosion rates. *Nat. Geosci.* **2025**, *18* (8), 732−739.
(72) Bhattacharya, A.; Bolch, T.; Mukherjee, K.; King, O.; Menounos, B.; Kapitsa, V.; Neckel, N.; Yang, W.; Yao, T. D. High Mountain Asian glacier response to climate revealed by multi-temporal satellite observations since the 1960s. *Nat. Commun.* **2021**, *12* (1), No. 4133.
(73) Kang, S.; Huang, J.; Wang, F.; Zhang, Q.; Zhang, Y.; Li, C.; Wang, L.; Chen, P.; Sharma, C. M.; Li, Q.; Sillanpaa, M.; Hou, J.; Xu, B.; Guo, J. Atmospheric Mercury Depositional Chronology Reconstructed from Lake Sediments and Ice Core in the Himalayas and Tibetan Plateau. *Environ. Sci. Technol.* **2016**, *50* (6), 2859−2869.
(74) Wang, X.; Luo, J.; Yuan, W.; Lin, C.-J.; Wang, F.; Liu, C.; Wang, G.; Feng, X. Global warming accelerates uptake of atmospheric mercury in regions experiencing glacier retreat. *Proc. Natl. Acad. Sci. U.S.A.* **2020**, *117* (4), 2049−2055.
(75) Carrivick, J. L.; Tweed, F. S. Deglaciation controls on sediment yield: Towards capturing spatio-temporal variability. *Earth-Sci. Rev.* **2021**, *221*, No. 103809.
(76) Wu, F.; Yang, L.; Wang, X.; Yuan, W.; Lin, C.-J.; Feng, X. Mercury Accumulation and Sequestration in a Deglaciated Forest Chronosequence: Insights from Particulate and Mineral-Associated Forms of Organic Matter. *Environ. Sci. Technol.* **2023**, *57* (43), 16512−16521.
(77) Su, F.; Zhang, L.; Ou, T.; Chen, D.; Yao, T.; Tong, K.; Qi, Y. Hydrological response to future climate changes for the major upstream river basins in the Tibetan Plateau. *Global Planet. Change* **2016**, *136*, 82−95.
(78) Zabel, N. A.; Hall, R. I.; Branfireun, B. A.; Swanson, H. K. Mercury accumulation in sediments of Lhu'aan Man' (Kluane Lake, YT): Response to past hydrological change. *Arct. Antarct. Alp. Res.* **2021**, *53* (1), 179−195.
(79) Søndergaard, J.; Tamstorf, M.; Elberling, B.; Larsen, M. M.; Mylius, M. R.; Lund, M.; Abermann, J.; Rigét, F. Mercury exports from a High-Arctic river basin in Northeast Greenland (74°N) largely controlled by glacial lake outburst floods. *Sci. Total Environ.* **2015**, *514*, 83−91.
(80) Sattar, A.; Haritashya, U. K.; Kargel, J. S.; Karki, A. Transition of a small Himalayan glacier lake outburst flood to a giant transborder flood and debris flow. *Sci. Rep.* **2022**, *12* (1), No. 12421.
(81) Zhang, T.; Li, D. F.; East, A. E.; Walling, D. E.; Lane, S.; Overeem, I.; Beylich, A. A.; Koppes, M.; Lu, X. X. Warming-driven erosion and sediment transport in cold regions. *Nat. Rev. Earth Environ.* **2022**, *3* (12), 832−851.
(82) Krause, V. M.; Baldwin, A. K.; Peterson, B. D.; Krabbenhoft, D. P.; Janssen, S. E.; Willacker, J. J.; Eagles-Smith, C. A.; Poulin, B. A. Riparian Methylmercury Production Increases Riverine Mercury Flux and Food Web Concentrations. *Environ. Sci. Technol.* **2024**, *58* (46), 20490−20501.
(83) Zhang, G. Q.; Carrivick, J. L.; Emmer, A.; Shugar, D. H.; Veh, G.; Wang, X.; Labedz, C.; Mergili, M.; Mölg, N.; Huss, M.; Allen, S.; Sugiyama, S.; Lützow, N. Characteristics and changes of glacial lakes and outburst floods. *Nat. Rev. Earth Environ.* **2024**, *5* (6), 447−462.
(84) Zheng, G. X.; Allen, S. K.; Bao, A.; Ballesteros-Cánovas, J. A.; Huss, M.; Zhang, G. Q.; Li, J. L.; Yuan, Y.; Jiang, L. L.; Yu, T.; Chen, W. F.; Stoffel, M. Increasing risk of glacial lake outburst floods from future Third Pole deglaciation. *Nat. Clim. Change* **2021**, *11* (5), 411−417.
(85) Hood, E.; Fellman, J.; Spencer, R. G. M.; Hernes, P. J.; Edwards, R.; D'Amore, D.; Scott, D. Glaciers as a source of ancient and labile organic matter to the marine environment. *Nature* **2009**, *462* (7276), 1044−1100.
(86) Luo, H.; Cheng, Q.; He, D.; Sun, J.; Li, J.; Pan, X. Recent advances in microbial mercury methylation: A review on methylation habitat, methylator, mechanism, and influencing factor. *Process Saf. Environ. Prot.* **2023**, *170*, 286−296.
(87) Ezzat, L.; Peter, H.; Bourquin, M.; Busi, S. B.; Michoud, G.; Fodelianakis, S.; Kohler, T. J.; Lamy, T.; Geers, A.; Pramateftaki, P.; Baier, F.; Marasco, R.; Daffonchio, D.; Deluigi, N.; Wilmes, P.; Styllas, M.; Schoen, M.; Tolosano, M.; De Staercke, V.; Battin, T. J. Diversity and biogeography of the bacterial microbiome in glacier-fed streams. *Nature* **2025**, *637* (8046), 622−630.
(88) Sun, X.; Zhang, Q.; Wang, J.; Zhang, B.; Guo, J.; Zhang, K.; Li, M.; Lu, Z.; Shi, J.; Kang, S. Emerging Proglacial Lake Constraints on Mercury Transport and Transform Patterns in Glacial Meltwater Runoff on the Tibetan Plateau. *J. Environ. Sci.* **2025**, DOI: 10.1016/j.jes.2025.10.009.
(89) Bosson, J. B.; Huss, M.; Cauvy-Fraunie, S.; Clement, J. C.; Costes, G.; Fischer, M.; Poulenard, J.; Arthaud, F. Future emergence of new ecosystems caused by glacial retreat. *Nature* **2023**, *620* (7974), 562−569.
(90) Mu, G.; Huang, M.; Wu, Z.; Cui, H.; Yang, Q.; Li, X.; Cui, X.; Tong, Y. Characteristics of nutrients and microbial communities in proglacial lakes on the Tibetan Plateau and their potential linkages associated with mercury. *J. Hazard. Mater.* **2025**, *492*, No. 138117.